Electronic Supplementary Material (ESI) for Nanoscale.
This journal is © The Royal Society of Chemistry 2023

Supplementary Information

Giant optical absorption of a $PtSe_2$-on-silicon waveguide in mid-infrared wavelengths

Tianping Xu,[a,b] Liqiang Qi,[a,b] Yingqi Xu,[c] Shuqi Xiao,[d] Quan Yuan,[a] Rui Niu,[a] Jiaqi Wang,*[c] Hon Ki Tsang,*[d] Tiegen Liu,[a,b] Zhenzhou Cheng *[a,b,e,f,g]

[a] School of Precision Instruments and Optoelectronics Engineering, Tianjin University, Tianjin 300072, China

[b] Key Laboratory of Optoelectronics Information Technology, Ministry of Education, Tianjin 300072, China

[c] College of Physics and Optoelectronic Engineering, Shenzhen University, Shenzhen 518060, China

[d] Department of Electronic Engineering, The Chinese University of Hong Kong, Shatin, Hong Kong

[e] Georgia Tech Shenzhen Institute, Tianjin University, Shenzhen 518055, China

[f] School of Physics and Electronic Engineering, Xinjiang Normal University, Urumqi, Xinjiang 830054, China

[g] Xinjiang Key Laboratory for Luminescence Minerals and Optical Functional Materials, Urumqi, Xinjiang 830054, China

*Corresponding author emails: jqwang@szu.edu.cn (J.Wang); hktsang@ee.cuhk.edu.cn (H. K Tsang); zhenzhoucheng@tju.edu.cn (Z. Cheng)

S1 Calculation of the complex dielectric constant of the ten-layer $PtSe_2$ film and the optical absorption of the $PtSe_2$-on-silicon waveguide

To obtain the complex dielectric constant of the ten-layer $PtSe_2$ film, we extracted ε_2 of a $PtSe_2$ film with a thickness of 6.1 nm according to the previous work [1]. Then, we used a Lorentz oscillator model to fit the data. Herein, the Lorentz oscillator model is given by $\varepsilon(E) = \frac{AE_0}{{E_0}^2 - E^2 - i\Gamma E} + eps$, where E_0 is the resonance energy, AE_0 is the oscillator strength, Γ is the damping constant, and eps is an offset parameter. To evaluate the fitting quality, a root mean square error was used in our method. With the parameters of A = 26.2 (eV), E_0 = 2.043 (eV), Γ = 0.6652 (eV), and eps = 0.7467, ε_2 exhibited the best fitting. Finally, ε_1 was calculated from ε_2 by using the Kramers-Kronig integrating, which is given by $\varepsilon_1(E) = \varepsilon_0 + \frac{2}{\pi} Q \int_{E_g}^{\infty} \frac{\zeta \varepsilon_2(\zeta)}{\zeta^2 - E^2} d\zeta$, where ε_0 is a fitting parameter, the Q represents the Cauchy principal part of the integral, and E_g is the photon energy. Based on the calculated complex dielectric constant, we can simulate the optical absorption of the $PtSe_2$-on-silicon waveguides. The optical absorption of $PtSe_2$ film on a 70-nm thick silicon waveguide achieves at least 2 times as high as that on a 220-nm thick silicon waveguide in our simulation, as shown in Fig. S1.

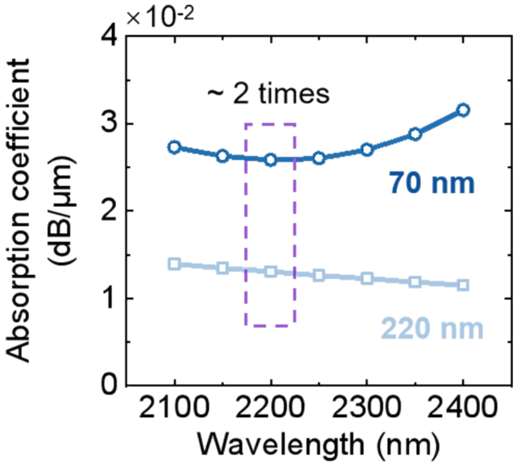

Fig. S1 Simulated optical absorption coefficients of $PtSe_2$-on-waveguides with the waveguide thicknesses of 70 nm and 220 nm.

S2 Device characterization

We used an optical microscope to characterize the morphology of $PtSe_2$ -on-silicon waveguides, as shown in Fig. S2(a). There is a clear difference in color before and after $PtSe_2$ transfer, as indicated in Fig. S2(b) and Fig. S2(c). The area of the $PtSe_2$ film we used is $1\ cm \times 1\ cm$, as shown in Fig. S2(d). Fig. S2(e) shows scanning electron microscopy (SEM) images of the waveguide cross-section.

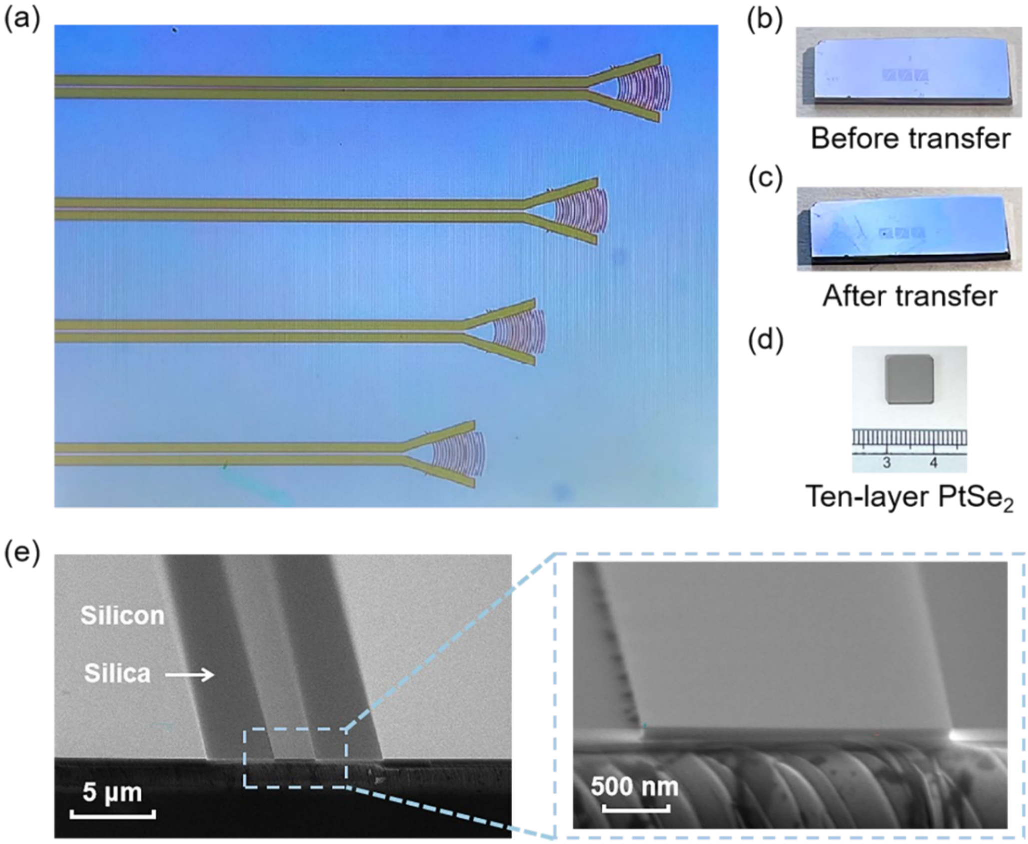

Fig. S2 Photographs of the silicon devices and $PtSe_2$ film. (a) Photographs of the $PtSe_2$ -on-silicon waveguides. Photographs of the silicon waveguides before (b) and after (c) the $PtSe_2$ film transfer. (d) Photograph of the $PtSe_2$ film grown on the silica substrate. (e) SEM images of the waveguide cross-section.

S3 Device testing system

The waveguide devices were measured by using a continuous-wave single-frequency tunable Cr2+: ZnS/Se laser (IPG CLT-2250-500). Ge-doped-silica-core optical fibers (Thorlabs SM2000) were used to couple the laser into and out of the $PtSe_2$ -on-silicon waveguide at an incident angle of 10°. A fiber polarization controller was used to control the polarization of the laser in the input fiber, while an InGaAs photodiode power meter (Thorlabs S148C) was used to detect the output power. Both the laser and the power meter were controlled using a Labview program.

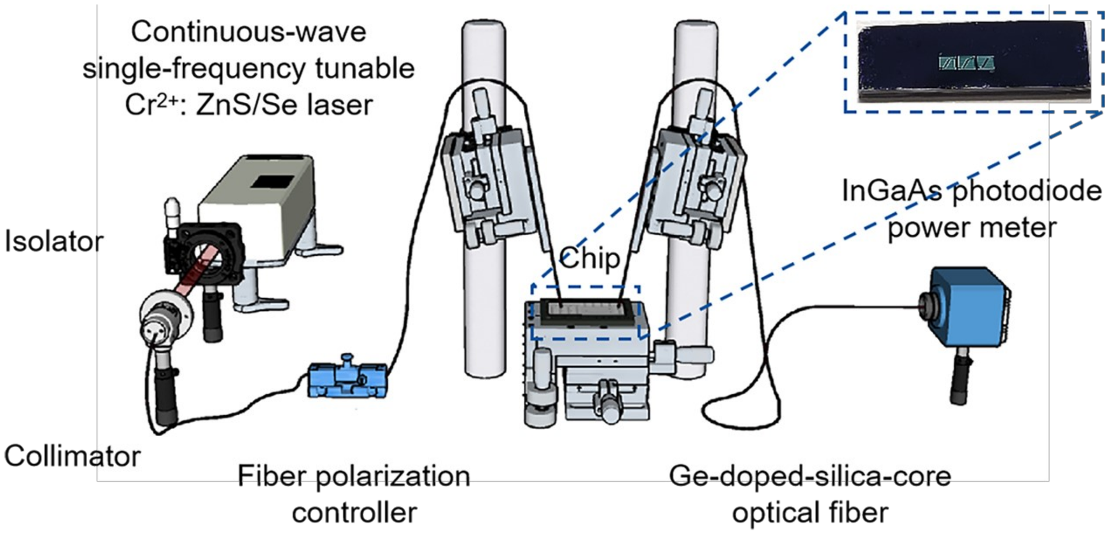

Fig. S3 Schematic of the device testing system.

S4 Simulation of the $PtSe_2$-on-silicon grating coupler

We simulated coupling spectra of the silicon grating coupler by using the three-dimensional finite-difference time-domain simulator. As shown in Fig. S4, the maximum coupling efficiency of the grating coupler was -8.4 dB. The center wavelength was shifted to long wavelengths by 23.77 nm (from 2190.18 nm to 2213.95 nm) with the presence of the $PtSe_2$ cladding, agreeing well with the experimental results. Moreover, the silicon grating coupler with the $PtSe_2$ film had a lower coupling efficiency than that without $PtSe_2$. This may be due to the reduction in the directionality of the ultra-thin silicon grating coupler and the introduction of absorption loss of $PtSe_2$, after integrating the $PtSe_2$ film on the chip surface.

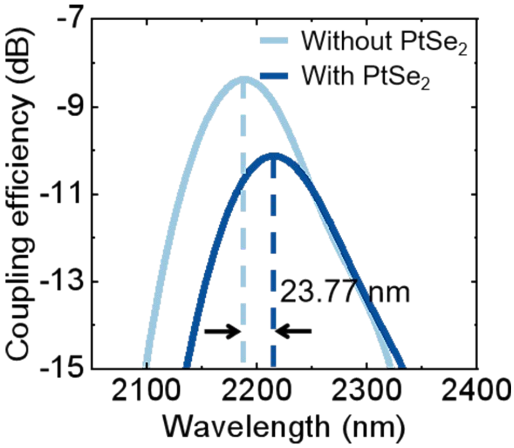

Fig. S4. Simulated coupling spectra of the grating coupler with and without the $PtSe_2$ film.

S5 Calculation of the optical loss coefficient of the microring resonator

After characterizing the transmission spectrum, the load Q factor (Q_L), free spectral range (*FSR*), and normalized transmission (*T*) can be obtained. The optical loss coefficient (α_0) can be calculated by using the equation [2], $\alpha_0 = \frac{\lambda_{res}}{\frac{2Q_L}{1+\sqrt{T}} \times FSR \times R}$, where *R* is the radius of the resonator, λ_{res} is the resonant wavelength.

Reference:

1 J. Xie, D. Zhang, X.-Q. Yan, M. Ren, X. Zhao, F. Liu, R. Sun, X. Li, Z. Li, S. Chen, Z.-B. Liu and J.-G. Tian, *2D Mater.*, 2019, **6**, 035011.

2 Y. Zhang, K. Zhong, G. Hu, D. Yi, R. R. Kumar and H. K. Tsang, *Applied Physics Letters*, 2020, **117**, 221103.